Exploring deep learning methods for characterizing near-source characteristics of buried explosions from seismic data

Jennifer L. Harding, Leiph A. Preston, Mehdi Eliassi

Sandia National Laboratories, Albuquerque, NM, USA

Sandia National Laboratories

INTRODUCTION AND MAIN RESULTS

We explore deep learning methods to characterize buried explosion emplacement using a large and growing dataset of simulated buried chemical explosions in a variety of subsurface ground materials with ranging material properties. Deep learning models are showing promising performance using the far-field seismic spectra to 25 Hz at the local scale, and are successfully validated using Blue Canyon Dome data.

Exploring deep learning methods for characterizing near-source characteristics of buried explosions from seismic data

Jennifer L. Harding[1], Leiph A. Preston[1], Mehdi Eliassi[1]

[1]Sandia National Laboratories, Albuquerque, New Mexico

T2.1-258

Motivation

- Physical characteristics at the source affect discriminants as well as source time function (STF) and yield estimates
- Machine learning (ML) can potentially learn these near-source characteristics from seismic data

Fig. 1: Local discriminant thresholds are affected by hard vs. soft rock

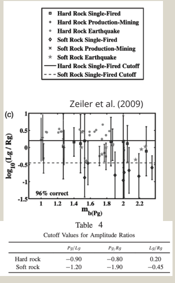

Fig. 2: STFs are affected by ground material and source emplacement

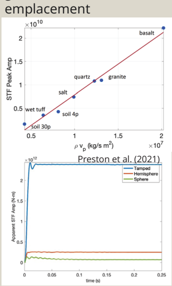

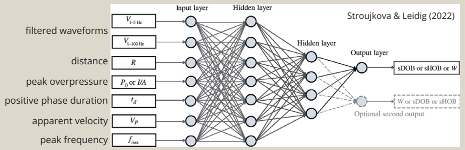

Fig. 3: ML can estimate depth of burial from far-field waveforms

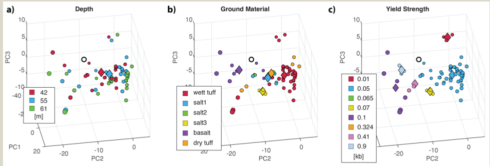

Fig. 4: Ground material and yield strength were shown to be more influential to far-field waveforms than depth in a set of simulations from better groupings in PCA space

Underground Explosion Simulations

- We use a nonlinear-to-linear modeling scheme to simulate buried explosions and their resultant far-field waveforms
- We vary the properties of a homogeneous half-space earth model:
- ground material
- yield strength
- fracture pressure
- source depth
- Poisson's ratio
- strength model and model parameters
- explosive mass and material

Fig.5: This diagram outlines our nonlinear-to-linear

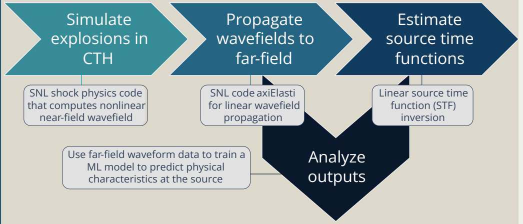

Far-Field Waveform Dataset

- We are generating a growing dataset consisting of far-field waveforms recording identical chemical explosion sources in a variety of subsurface models
- We will look at 551 simulations and focus on ground material and emplacement (cavity vs. tamped)

Data Distribution

Placement	Basalt	Dry Tuff	Salt1	Salt2	Wet Tuff
Cavity	0.22	0.21	0	0	0.0073
Tamped	0.14	0.088	0.081	0.095	0.16

EOS

Fig.6: We are working on balancing the

- 2-channel waveforms record vertical and radial velocity (axi-symmetric simulations) and are filtered to 0.001 - 4,500 Hz and resampled to a sample rate of 10,000 Hz
- We output discrete frequencies to 750 Hz using a fast Fourier transform
- features are de-meaned and normalized

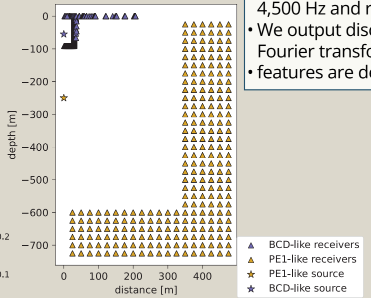

Fig.7: We have two types of simulations with different source depths and receiver locations based on two different tests conducted at NNSS. The majority of simulations are at the BCD-like scale.

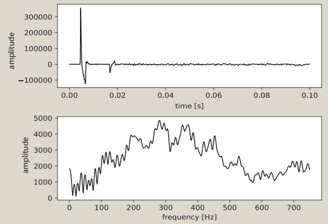

Fig.8: The top panel shows the filtered and resampled far-field particle velocities from a BCD-like simulation and the bottom panel shows the spectra to 750 Hz.

Deep Learning Methods

- We explore fully connected neural network (FCNN) and convolutional neural network (CNN) architectures to classify emplacement and ground material

- We split the input data into a train and validation set (80/20), keeping the samples from each simulation case together, either in the train or validation set
- We use k-fold cross validation to compare model performance with k=5
- We use a batch size of 400 and train for 200 epochs
- Training each model takes between 10 and 45 min. on an NVIDIA V100S-Q 4 GiB GPU, depending on the number of trainable parameters and input data size

- We use the NeuralSens package (Pizarroso et al., 2022) to perform sensitivity analysis on trained FCNNs
- This is a good tool for better understanding and trusting the ML model and evaluating feature importance

Sensitivity Metrics

mean sensitivity: $$S_{ik}^{avg} = \frac{\sum_{j=1}^{N} s_{ik}|_{x_j}}{N}$$

sensitivity standard deviation: $$S_{ik}^{sd} = \sigma\left(s_{ik}|_{x_j}\right); j \in 1, \ldots, N$$

mean squared sensitivity: $$S_{ik}^{sq} = \sqrt{\frac{\sum_{j=1}^{N}\left(s_{ik}|_{x_j}\right)^2}{N}}$$

k: output neuron; x: training samples; i: input variable; N number of j samples

a) "Baseline" FCNN Architecture

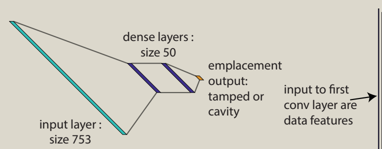

b) "Baseline" CNN Architecture

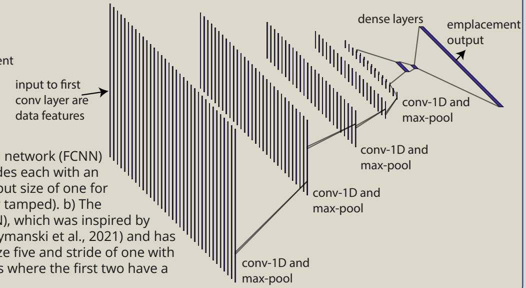

Fig.9: a) The baseline fully-connected neural network (FCNN) architecture, which has two layers of 50 nodes each with an input layer of 753 data features and an output size of one for emplacement binary classification (cavity or tamped). b) The baseline convolutional neural network (CNN), which was inspired by X-ray diffraction models from chemistry (Szymanski et al., 2021) and has six layers with 1-D convolutions of kernel size five and stride of one with max-pooling, followed by three dense layers where the first two have a dropout rate of 5%.

Sensitivity analysis results for the baseline FCNN

Fig.10: These plots show the mean (top), standard deviation (middle) and mean squared (bottom) sensitivity of the emplacement output to the input features using 5,000 random input training samples and the trace-shuffled baseline FCNN model. The mean squared sensitivity can be interpreted as feature importance. Lower frequencies are more important than higher. We use these plots to test model performance when the input spectra are limited to lower frequencies using different high-frequency cutoffs.

Preliminary Results: Emplacement Classification

Baseline model comparisons

	# train. params	train mean accuracy	train mean loss	val. mean accuracy	val. mean loss	val. mean precision	val. mean recall	val. mean f1	mean BCD class
baseline CNN	1.8e+04	0.99	0.025	0.95	0.21	0.95	0.94	0.94	0.87
baseline FCNN	4e+04	0.99	0.018	0.96	0.34	0.97	0.93	0.95	0.83

Fig.11: Results from training the baseline FCNN and CNN models with the full input spectra to 750 Hz, with darker colors highlighting better model performance metrics. Blue colors show percentage-based metrics, teal colors show losses, and orange colors show the number of trainable parameters. The true BCD class is 1(tamped).

Baseline models with reduction of higher input frequencies

	# train. params	train mean accuracy	train mean loss	val. mean accuracy	val. mean loss	val. mean precision	val. mean recall	val. mean f1	mean BCD class
baseline CNN 25 Hz	1.8e+04	0.87	0.29	0.8	0.58	0.84	0.76	0.8	0.92
baseline CNN 75 Hz	1.8e+04	0.95	0.15	0.87	0.36	0.86	0.85	0.86	0.87
baseline FCNN 75 Hz	6.6e+03	0.95	0.13	0.91	0.46	0.89	0.9	0.89	1
baseline FCNN 150 Hz	1e+04	0.98	0.066	0.94	0.23	0.95	0.92	0.93	0.99
baseline FCNN 250 Hz	1.5e+04	0.99	0.03	0.95	0.31	0.94	0.95	0.95	0.98

Fig.12: Results from training the baseline FCNN and CNN models with limited higher frequencies, where darker colors highlighting better model performance metrics. Blue colors show percentage-based metrics, teal colors show losses, and orange colors show the number of trainable parameters. The true BCD class is 1(tamped).

Improving 25 Hz model architectures

	# train. params	train mean accuracy	train mean loss	val. mean accuracy	val. mean loss	val. mean precision	val. mean recall	val. mean f1	mean BCD class
	~~9.7e+03~~	~~0.9~~	~~0.23~~	~~0.84~~	~~0.39~~	~~0.8~~	~~0.81~~	~~0.81~~	0.67
CNNs	2e+04	0.92	0.19	0.85	0.84	0.84	0.8	0.82	1
	1.8e+04	0.9	0.21	0.85	0.73	0.85	0.82	0.83	1
CNN: 1 conv layer size 25, kernel=3; 3 dense layers size 50	2.2e+04	0.9	0.22	0.85	0.48	0.83	0.82	0.83	1
	1e+04	0.92	0.17	0.84	0.52	0.86	0.78	0.82	1
CNN: 3 conv layers size 25, kernel=3; 2 dense layers size 50	7.8e+03	0.91	0.21	0.83	0.58	0.86	0.8	0.83	1
FCNNs — FCNN: 4 layers; 100 nodes each	3.3e+04	0.95	0.1	0.89	1.2	0.89	0.86	0.88	0.98
	9.2e+03	0.93	0.16	0.87	0.74	0.88	0.82	0.85	0.99
	2.3e+04	0.94	0.13	0.88	0.85	0.89	0.84	0.86	1
	4.6e+04	0.95	0.11	0.87	2.4	0.85	0.87	0.85	1
	5.8e+04	0.95	0.11	0.88	1.1	0.86	0.87	0.86	1
FCNN: 3 layers; 300, 150, 25 nodes	5.8e+04	0.94	0.12	0.88	2	0.88	0.87	0.87	1
	1.8e+04	0.93	0.14	0.88	0.86	0.87	0.86	0.86	0.99
	1.7e+04	0.91	0.2	0.87	0.98	0.86	0.86	0.86	0.97

Fig.13: Results from training other FCNN and CNN architectures, four of which are labeled to the left. We improve performance for models with 25 Hz cutoffs by using different numbers of dense and convolutional layers and layer sizes, as well as convolutional filter kernel sizes (all strides are 1). FCNN models outperform CNN models, but further exploration and hyperparameter optimization is needed when the full dataset is generated. Blue colors show percentage-based metrics, teal colors show losses, and orange colors show the number of trainable parameters. The true BCD class is 1(tamped).

Summary

- Emplacement classification shows promising performance, even for lower-frequency input spectra

Ongoing Work and Future Directions

- Model architecture and hyperparameter optimization once the full dataset is generated
- Explore other input data processing or modes
- Look into other testing datasets
- Classify other near-source characteristics and add other characteristics to CTH modeling (e.g., porosity)
- Classify cavity features like shape and size
- Develop larger-scale capabilities (from local to regional)

Acknowledgments

The authors would like to Acknowledge Andréa Darrh for their technical review of this poster. This Low Yield Nuclear Monitoring (LYNM) research was funded by the National Nuclear Security Administration, Defense Nuclear Nonproliferation Research and Development (NNSA DNN R&D). The authors acknowledge important interdisciplinary collaboration with scientists and engineers from LANL, LLNL, NNSS, PNNL, and SNL.

References

Pizarroso, J., Portela, J., & Muñoz, A. (2022). NeuralSens: Sensitivity Analysis of Neural Networks. Journal of Statistical Software, 102(7). doi:10.18637/jss.v102.i07

Preston, L., Eliassi, M., & Poppeliers, C. (2021). Programmatic advantages of linear equivalent seismic models (No. SAND2021-10201). Sandia National Lab.(SNL-NM), Albuquerque, NM (United States).

Stroujkova, A., & Leidig, M. (2022). Using machine learning for explosion yield estimation. Bulletin of the Seismological Society of America, 112(3), 1397-1415.

Szymanski, N. J., Bartel, C. J., Zeng, Y., Tu, Q., & Ceder, G. (2021). Probabilistic Deep Learning Approach to Automate the Interpretation of Multi-phase Diffraction Spectra. Chemistry of Materials, 33(11), 4204-4215. doi:10.1021/acs.chemmater.1c01071

Zeiler, C., & Velasco, A. A. (2009). Developing local to near-regional explosion and earthquake discriminants. Bulletin of the Seismological Society of America, 99(1), 24-35.

Sandia National Laboratories is a mutimission laboratory managed and operated by National Technology & Engineering Solutions of Sandia, LLS, a wholly owned subsidiary of Honeywell International Inc., for the U.S. Department of Energy's National Nuclear Security Administration under contract DE-NA0003525.
SAND No.